Transient picosecond Raman studies of electron and hole velocity overshoots in a GaAs-based p–i–n semiconductor nanostructure

2005 J. Phys.: Condens. Matter 17 1679

(http://iopscience.iop.org/0953-8984/17/10/021)

INSTITUTE OF PHYSICS PUBLISHING JOURNAL OF PHYSICS: CONDENSED MATTER

J. Phys.: Condens. Matter **17** (2005) 1679–1686 doi:10.1088/0953-8984/17/10/021

Transient picosecond Raman studies of electron and hole velocity overshoots in a GaAs-based p–i–n semiconductor nanostructure

W Liang[1], K T Tsen[1], C Poweleit[1], J M Barker[2], D K Ferry[2] and H Morkoc[3]

[1] Department of Physics and Astronomy, Arizona State University, Tempe, AZ 85281, USA
[2] Department of Electrical Engineering, Arizona State University, Tempe, AZ 85287, USA
[3] Department of Electrical Engineering, Virginia Commonwealth University, Richmond, VA 23284, USA

Received 9 November 2004, in final form 2 February 2005
Published 25 February 2005
Online at stacks.iop.org/JPhysCM/17/1679

Abstract

We report the observation of a velocity overshoot phenomenon for electrons as well as holes in a GaAs-based p–i–n nanostructure by using transient picosecond Raman spectroscopy. Under the picosecond laser excitation, we have found that the extent of velocity overshoot for electrons is comparable to that of holes. These experimental results have been explained in terms of various carrier scattering processes. Comparisons with results obtained from other III–V semiconductors are also made and a comprehensive discussion is given.

(Some figures in this article are in colour only in the electronic version)

1. Introduction

Recent progress in microelectronic fabrication processing has brought the size of electronic devices down to the order of 0.1 μm or smaller. This means that a very strong electric field intensity exists in such an electronic device if an operation voltage (which is of the order of 1 V) is applied. The transport properties of the charge carriers, electrons and holes, are determined by many factors; among them, electric field intensity plays an important role. Under very high electric field intensity, the carrier transient transport phenomenon, which normally lasts for one picosecond or less, has been demonstrated to exhibit drastically different behaviour from that of the steady state [1–5].

There are two important transient transport phenomena: ballistic transport and velocity overshoot. The former corresponds to a transport phenomenon in which electrons travel with minimal scattering; the latter represents a transport phenomenon where the electron drift velocity is substantially higher than its steady state value. These transient transport phenomena have recently attracted a lot of attention because of their potential in greatly enhancing the performance of an electronic device. In this paper, we report the observation of the velocity

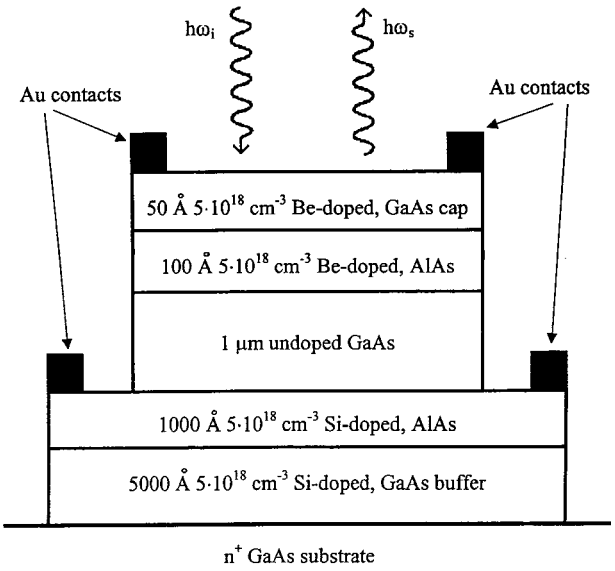

Figure 1. GaAs-based p–i–n nanostructure sample used in the transient carrier transport experiments.

overshoot phenomenon for electrons as well as holes in a GaAs-based p–i–n nanostructure by using transient picosecond Raman spectroscopy.

2. Samples and experimental technique

The GaAs-based p–i–n nanostructure used in this work is shown in figure 1. It is an AlAs–GaAs–AlAs p–i–n nanostructure grown by molecular beam epitaxy on a (001)-oriented GaAs substrate. The p-type region is made up of a 100 Å thick Be-doped ($\cong 5 \times 10^{18}$ cm^{-3}) AlAs layer and a 50 Å thick Be-doped ($\cong 5 \times 10^{18}$ cm^{-3}) GaAs cap layer. The i-region is a 1 μm thick intrinsic GaAs layer. This is the active region probed by our Raman scattering experiments. The n-type region consists of a 1000 Å thick Si-doped ($\cong 5 \times 10^{18}$ cm^{-3}) AlAs layer and a 5000 Å thick Si-doped ($\cong 5 \times 10^{18}$ cm^{-3}) GaAs buffer layer. Gold contacts are established on both the p and n sides of the mesa-like p–i–n diode structure in order to apply an electric field. An opening of $\cong 0.25$ mm^2 in area is created in the gold layer on the p side of the diode so that light scattering experiments can be carried out. The Be-doped p-type layer and Si-doped n-type layer serve as a capacitor and provide a uniform electric field across the active region of the sample.

Raman spectroscopy has been proven to be a viable technique to probe electron dynamics in semiconductors [6]. Here, transient Raman spectroscopy is employed to directly measure electron distribution function. The excitation laser having photon energy larger than the bandgap of GaAs is incident upon the intrinsic region of GaAs to generate electron–hole pairs. These hot carriers, which drift in opposite directions due to the application of an electric field, are then probed by the trailing portion of the same laser by Raman spectroscopy. Since the same laser pulse is used for both excitation and probing, our experimental results represent an average over the duration of the pulse. The single-particle scattering (SPS) cross section is proportional to the projection of the electron velocity distribution along the wavevector transfer direction [7]; as a result, if the experimental configuration is chosen such that the wavevector

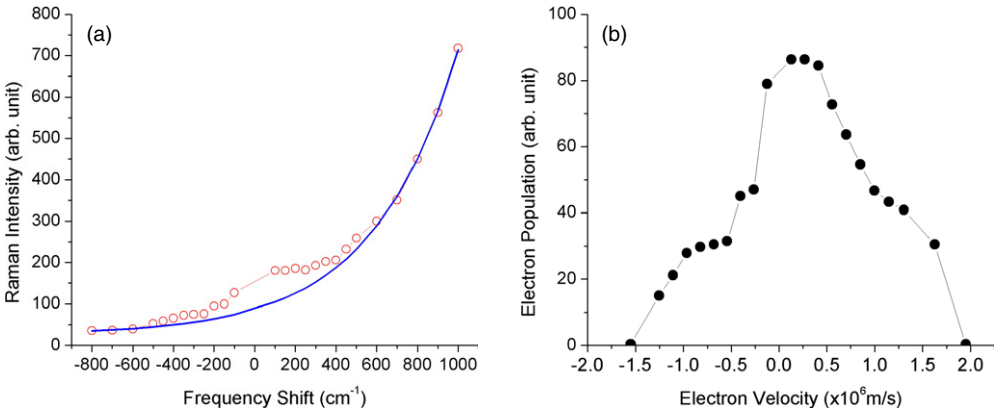

Figure 2. (a) A typical SPS spectrum taken for a GaAs-based p–i–n nanostructure, with 2 ps excitation laser pulse width and for an electron–hole pair density of 5×10^{17} cm^{-3}. The open circles are data. The solid curve corresponds to the best-fit exponential function. (b) The electron distribution obtained from the SPS spectrum of (a) after the background subtraction.

transfer direction is parallel to the applied electric field direction the electron transport can be directly measured. Furthermore, we notice that the SPS cross section is inversely proportional to the square of the effective mass of the carrier. Since in a typical semiconductor such as GaAs the effective mass of a hole is about one order of magnitude larger than that of an electron, Raman scattering preferentially detects electron distribution even if the electron and hole are simultaneously present. The transient hole distribution, however, can be indirectly deduced by measuring the electron–hole pair luminescence spectrum together with the electron distribution.

The excitation source is a DCM dye laser, which is synchronously pumped by the second harmonic of a cw mode-locked YAlG laser. The laser has a repetition rate of 76 MHz; its pulse width is tuned to either 2 ps or 20 ps, depending on the experimental needs. The laser photon energy is about $\hbar\omega = 2.0$ eV. The $Z(X, Y)\bar{Z}$ scattering configuration is used, where $X = (100)$, $Y = (010)$, $Z = (001)$, so that SPS associated with spin-density fluctuations can be detected [8–10]. All the experimental results were obtained at $T = 300$ K.

3. Experimental results and analysis

Figure 2(a) shows a typical SPS spectrum for the GaAs-based p–i–n nanostructure, taken with an excitation laser having a pulse width of 2 ps. The injected electron–hole pair density is estimated to be $n \cong 5 \times 10^{17}$ cm^{-3}. The effective applied electric field intensity is about 10 kV cm^{-1}. The SPS spectrum has been found to sit on a smooth luminescence background coming from the hot electron–hole recombination associated with the E_0 bandgap of GaAs. This luminescence background has been found to be very well fitted by an exponential curve within the range of frequency shift of our interest, i.e., from -800 to 1000 cm^{-1} [11, 12].

In order to experimentally justify the validity of this exponential background subtraction, we have measured the SPS spectrum under a very tight laser focusing condition so that the excited electron–hole pair density is about 1.5×10^{19} cm^{-3}, as shown in figure 3. Under our single-pulse excite and probe experiments, if one varies the size of the focused spot on the sample while keeping the laser intensity constant, the luminescence intensity should scale with the square of the excitation laser power density, whereas the SPS contribution is expected

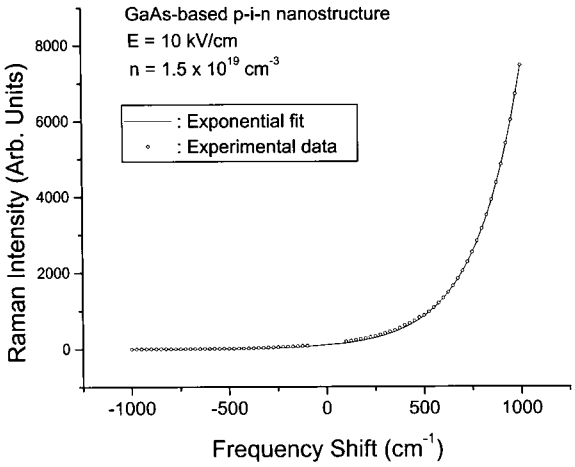

Figure 3. A Raman scattering spectrum taken for a GaAs-based p–i–n nanostructure with extremely high photoexcited electron–hole pair density of 1.5×10^{19} cm^{-3}. The spectrum should be dominated by the luminescence contributions. The solid curve represents an exponential fit for the data. This results verifies the way the background subtraction has been handled in our experimental analysis.

to remain constant; as a result, for sufficiently tight focusing (i.e., sufficiently high excited electron–hole pair density) such as that shown in figure 3, the Raman scattering spectrum is expected to be dominated by the luminescence signal. The fact that the Raman spectrum in figure 3 can be very well fitted by an exponential function for the spectral range indicated strongly supports the way we carry out the background subtraction.

After the subtraction of the luminescence background, the subtracted spectrum is then transformed into the electron velocity distribution [13], which is shown in figure 2(b). In making the conversion the correction for the effects of non-parabolicity of the conduction band has been taken into account with the help of pseudopotential calculations of Cohen *et al* [14] for GaAs. It is clear from figure 2(b) that the electron distribution is shifted toward the opposite direction of the applied electric field, as expected. The electron distribution mimics a Maxwell–Boltzmann distribution due to the fact that a relatively long ($\simeq$2 ps) laser pulse is used in the experiment. The electron drift velocity in this case is deduced to be $V_{\rm de} = (2.5 \pm 0.3) \times 10^7$ cm s^{-1}.

The corresponding E_0 bandgap luminescence spectrum is shown in figure 4(a) for the applied electric field intensity of $E = 10$ kV cm^{-1}. The intensity of luminescence $L(E_{\rm a})$ due to electron–hole pair recombination can be shown to be given by [15]

$$L(E_{\rm a}) = C{\rm e}^{-(\beta_{\rm e}a_{\rm e}+\beta_{\rm h}a_{\rm h})E_{\rm a}} \int_{-k_a}^{k_a} {\rm d}k_z\, q_{\rm e}(k_z) q_{\rm h}(k_z) {\rm e}^{(\beta_{\rm e}a_{\rm e}+\beta_{\rm h}a_{\rm h})E^{\mu}(k_z)} \tag{1}$$

where C is a constant;

$$\beta_{\rm e} = 1/k_{\rm B}T_{\rm e}; \qquad \beta_{\rm h} = 1/k_{\rm B}T_{\rm h};$$
$$a_{\rm e} = m_{\rm h}^*/(m_{\rm e}^* + m_{\rm h}^*);$$
$$a_{\rm h} = m_{\rm e}^*/(m_{\rm e}^* + m_{\rm h}^*);$$

$k_{\rm B}$ is the Boltzmann constant; $T_{\rm e}$ and $T_{\rm h}$ are electron and hole temperatures in the x–y directions; $m_{\rm e}^*$ and $m_{\rm h}^*$ are the effective masses of the electron and heavy hole, respectively;

$$E_{\rm a} \equiv E - E_{\rm g};$$
$$E^{\mu}(k) \equiv E_{\rm e}(k) + E_{\rm h}(k);$$

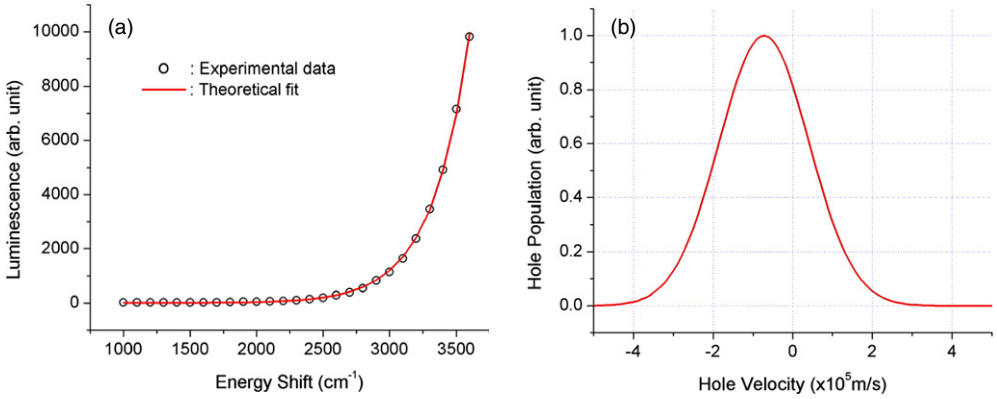

Figure 4. (a) Luminescence intensity (open circles) fitted by equation (1) (solid curve) with hole distribution as a fitting parameter. (b) The hole distribution obtained from the fit.

$$E_e = \hbar k_e^2/2m_e^*$$
$$E_h = \hbar k_h^2/2m_h^*$$
$$E = E_e + E_h + E_g;$$

$\vec{k}_e$ and $\vec{k}_h$ are the wavevectors of the electron and hole, respectively; E_g is the bandgap and E is the luminescence energy from electron and hole recombination; $k_a \equiv \sqrt{2\mu E_a}/\hbar$, where $1/\mu \equiv 1/m_e^* + 1/m_h^*$; and $q_e(k_z)$ and $q_h(k_z)$ are the electron and hole distributions in the z-direction, respectively.

Equation (1) states that the hole distribution along the wavevector transfer direction (in this case, the z-direction) can be deduced once the electron distribution along the wavevector transfer direction and the luminescence intensity of electron–hole pair recombination are determined.

Since the hole distribution appearing in equation (1) is under the integral sign, in principle, the hole distribution might not be deduced uniquely. However, we notice that in our experiments

(1) the photoexcited electron–hole pair density is relatively high ($n \cong 5 \times 10^{17}$ cm^{-3}); as a result, momentum randomization is expected to be quite efficient, as evidenced by the observation that electron distribution resembles a Maxwell–Boltzmann distribution function (figure 2(b));
(2) the hole has a very large effective mass ($\cong 0.45\, m_e$). Consequently, we expect that the hole distributions under our experimental conditions should be very well described by a shifted Fermi–Dirac function determined completely by two parameters: the hole temperature T_{hz} and the hole drift velocity V_{dh}.

Figure 4(a) shows the electron–hole pair luminescence spectrum and its fit by equation (1) for the laser pulse width of 2 ps. The parameter set best fitting our data is $T_h = (315 \pm 30)$ K, $T_{hz} = (330 \pm 30)$ K, $V_{dh} = (7.2 \pm 0.7) \times 10^6$ cm s^{-1}. The deduced hole distribution along the wavevector transfer direction or z-direction is shown in figure 4(b).

We have also carried out similar experiments on the sample except that the laser pulse width is $\cong$20 ps (which is not shown here). The electron drift velocity has been found to be $V_{de} = (1.5 \pm 0.2) \times 10^7$ cm s^{-1}. The parameter set best fitting the electron–hole pair luminescence is $T_h = (300 \pm 30)$ K, $T_{hz} = (300 \pm 30)$ K, $V_{dh} = (4.0 \pm 0.4) \times 10^6$ cm s^{-1}. For the sake of clarity, all the experimental results are summarized in table 1. Since experimental

Table 1. Drift velocities of electrons and holes obtained by excitation laser pulses of different durations for a GaAs p–i–n nanostructure.

	Laser pulse width	
Drift velocity	2 ps	20 ps
V_{de} (cm s^{-1})	$(2.5 \pm 0.3) \times 10^7$	$(1.5 \pm 0.2) \times 10^7$
V_{dh} (cm s^{-1})	$(7.2 \pm 0.7) \times 10^6$	$(4.0 \pm 0.4) \times 10^6$

results for a laser pulse width as long as 20 ps represent very closely the steady-state value, based upon results in table 1, we conclude that electron and hole velocity overshoots have been observed and demonstrated in our experiments.

4. Discussion

We notice that in order to use equation (1) to deduce the hole distribution one has to make sure that the electron–hole luminescence lasts sufficiently shorter than the laser pulse width. We estimate that the penetration depth for the photon energy used in the experiments is about 3000 Å. Since the combined electron and hole drift velocities are 3.0×10^7 and 2.0×10^7 cm s^{-1} for the excitation pulse widths of 2 and 20 ps, respectively, the electron–hole luminescence lasts significantly shorter than the corresponding excitation pulse width. As a result the luminescence may be regarded as essentially coincident with the excitation laser pulse.

The different response of the electrons and the holes under applied electric field can be understood by the nature of the scattering process different carrier undergoes. For the electrons, they are rapidly accelerated in the field to higher energies, subsequently scattered from Γ valley to the L and X valleys of the conduction band. This process is very efficient, and within a short time period (∼1.0 ps) those carriers at a higher energy position in the Γ valley can be monitored. Experimentally, we observe the velocity overshoot. On the other hand, for a longer period of time (about the order of 20 ps), the electrons in the Γ valley are mostly those returned from the satellite valleys. Those electrons have been randomized efficiently due to the inter- and intra-valley scattering processes [16]. Hence more low energy electrons, compared with the energetic ones, weigh in the electron distribution, and we expect a much lower drift velocity on this timescale. The data in table 1 indicate this is exactly the case. The electron drift velocity overshoots its steady-state value by a factor of about 1.7. We attribute this small electron overshoot factor to the relatively long laser pulse width ($\widetilde{=}$2 ps) used in our experiments.

On the other hand, inter-valley scattering for the holes is not phenomenal, due to both the valence band structure of GaAs and the effective mass of the hole. There is scattering between different hole bands, specifically with the anisotropic nature of the bands. Nevertheless, the dominant scattering process is intra-Γ-valley TO modes [17]. This process is ultrafast, and as a result the hole drift velocity overshoots its steady-state value by a factor of about 1.8.

Carrier drift velocity in direct bandgap semiconductors is affected by several factors, such as inter-valley scattering and intra-valley scattering processes, alloy scattering processes, carrier effective mass, energy separation between the gamma and satellite valleys, and the excess energy of the electrons above the conduction band minimum. In general, carrier effective mass and alloy scattering processes are most important in the determination of steady-state carrier drift velocity, whereas inter-valley and intra-valley scattering processes, energy difference between gamma and satellite valleys, and excitation photon energies are most effective in determining carrier transient drift velocity under the ultrashort pulse excitation.

It is very interesting to compare our present results with those obtained for an $Al_{0.3}Ga_{0.7}As$-based p–i–n nanostructure [18]. One would expect that because of the effects of alloy scattering and larger electron effective mass, $Al_{0.3}Ga_{0.7}As$ would have a smaller quasi-steady-state electron drift velocity (which is deduced from long-pulse laser excitations) than GaAs at comparable applied electric field intensities. This is indeed observed in our experimental observations—the electron drift velocities are $(1.5 \pm 0.2) \times 10^7$ cm s^{-1} and $(9.0 \pm 0.9) \times 10^6$ cm s^{-1} for GaAs and $Al_{0.3}Ga_{0.7}As$, respectively. On the other hand, the transient electron drift velocity observed for $Al_{0.3}Ga_{0.7}As$ ($V_e = (6.7 \pm 0.6) \times 10^7$ cm s^{-1}) has been found to be significantly larger than that for GaAs ($V_e = (2.5 \pm 0.3) \times 10^7$ cm s^{-1}). We attribute this difference to the electron velocity overshoot effects. The pulse width of the excitation laser used in the studies of $Al_{0.3}Ga_{0.7}As$ is about 0.8 ps, which is comparable to the inter-valley scattering time of $Al_{0.3}Ga_{0.7}As$, as a result the observed transient electron drift velocity is greatly enhanced, whereas a 2 ps laser pulse is used in the investigations of GaAs, which makes the effect of electron velocity overshoot relatively ineffective.

For holes, the situation is a little bit different. Because of the extremely fast (of the order of 100 fs) intra-valley TO phonon scattering, the effect of hole velocity overshoot lasts for a relatively shorter time than electrons. In addition, the hole effective masses in GaAs and $Al_{0.3}Ga_{0.7}As$ are very similar. These facts explain why the observed hole drift velocity under the 2 ps laser excitation for GaAs ($V_h = (7.2 \pm 0.7) \times 10^6$ cm s^{-1}) is found to be comparable to that under the 0.8 ps laser excitation for $Al_{0.3}Ga_{0.7}As$ ($V_h = (7.1 \pm 0.7) \times 10^6$ cm s^{-1}). On the other hand, the experimental results indicate that the quasi-steady-state hole velocity for GaAs ($V_h = (4.0 \pm 0.4) \times 10^6$ cm s^{-1}) is slightly larger than that for $Al_{0.3}Ga_{0.7}As$ ($V_h = (3.0 \pm 0.3) \times 10^6$ cm s^{-1}), a result which is most likely due to the effect of alloy scattering associated with the latter.

We note that the value of electron drift velocity obtained for $Al_{0.3}Ga_{0.7}As$ ($V_e = (6.7 \pm 0.6) \times 10^7$ cm s^{-1}) has been found to be significantly larger than those of GaAs ($V_e = (3.2 \pm 0.3) \times 10^7$ cm s^{-1}), InP ($V_e = (4.0 \pm 0.4) \times 10^7$ cm s^{-1}) and $In_{0.53}Ga_{0.47}As$ ($V_e = (5.4 \pm 0.5) \times 10^7$ cm s^{-1}) [19]. We attribute this result to the difference in the injection of photoexcited electrons. In the former, the photoexcited electrons were injected very close to the bottom of the conduction band; the electrons can therefore be accelerated for a longer time before suffering the Γ to X or Γ to L inter-valley scattering; in other words, electron velocity overshoot lasts significantly longer.

5. Conclusion

Electron and hole velocity overshoot in a GaAs-based p–i–n nanostructure are directly observed by picosecond Raman spectroscopy. We have found that the extent of velocity overshoot for electrons is comparable to holes. The experimental results are discussed and explained in terms of electron and hole scattering processes in GaAs. Comparisons with results obtained from other III–V semiconductors are made and comprehensive discussions are given.

Acknowledgment

This work is supported by the National Science Foundation under grant No DMR-0305147.

References

[1] Ferry D K, Grubin H L and Iafrate G J 1984 *Semiconductors Probed by Ultrafast Laser Spectroscopy* vol 1, ed R R Alfano (New York: Academic) p 413

[2] Constant E 1985 *Hot Electron Transport in Semiconductors* (*Springer Topics in Applied Physics* vol 58) ed L Reggiani (Berlin: Springer) p 227
[3] Shah J and Leheny R F 1984 *Semiconductors Probed by Ultrafast Laser Spectroscopy* vol 1, ed R R Alfano (New York: Academic) p 45
[4] Tsen K T 2001 *Ultrafast Phenomena in Semiconductors* ed K T Tsen (New York: Springer) p 191
[5] Tsen K T 2004 *Ultrafast Dynamical Processes in Semiconductors* (*Springer Topics in Applied Physics* vol 92) ed K T Tsen (Heidelberg: Springer) p 193
[6] Klein M V 1983 *Light Scattering in Solids I* (*Springer Topics in Applied Physics* vol 8) ed M Cardona (New York: Springer) p 151
[7] Hamilton D C and McWhorter A L 1969 *Light Scattering Spectra of Solids* ed G Wright (New York: Springer) p 309
[8] Chia C, Sankey O F and Tsen K T 1992 *Phys. Rev.* B **45** 6509
[9] Chia C, Sankey O F and Tsen K T 1992 *J. Appl. Phys.* **72** 4325
[10] Chia C, Sankey O F and Tsen K T 1993 *Mod. Phys. Lett.* B **7** 331
[11] Kim D S and Yu P Y 1990 *Light Scattering in Semiconductor Structures and Superlattices* (*NATO ASI Series* vol 273) ed D J Lockwood and J F Young p 383
[12] Grann E D, Sheih S J, Tsen K T, Sankey O F, Guncer S E, Ferry D K, Salvador A, Botcharev A and Morkoc H 1995 *Phys. Rev.* B **51** 1631
[13] Grann E D, Tsen K T, Ferry D K, Salvador A, Botcharev A and Morkoc H 1996 *Phys. Rev.* B **53** 9838
[14] Cohen M L and Chelikowsky J R 1988 *Electronic Strucuture and Optical Properties of Semiconductors* (Berlin: Springer) pp 102–12
[15] Chen Y, Tsen K T, Sankey O F and Ferry D K 2001 *Phys. Rev.* B **64** 195331
[16] Joshi R P, Grondin R O and Ferry D K 1990 *Phys. Rev.* B **42** 5685
[17] Joshi R P and Ferry D K 1989 *Phys. Rev.* B **39** 1180
[18] Wei W, Lee H, Tsen K T, Sankey O F and Ferry D K 2002 *Appl. Phys. Lett.* **81** 3999
[19] Liang W, Tsen K T, Ferry D K, Wu M-C, Ho C-C and Ho W-J 2003 *Appl. Phys. Lett.* **83** 1438